J. Fluid Mech. (1970), *vol.* 41, *part* 3, *pp.* 641–652
Printed in Great Britain

Unsteady flow of a viscous fluid from a source in a wall

By E. O. TUCK

Department of Mathematics, University of Adelaide

(Received 13 March 1969)

A problem with possible physiological applications concerns the escape of a viscous fluid through a small hole in a wall. The solution presented here is for a line source of sinusoidally pulsating strength located at the origin $x = y = 0$, where the plane $y = 0$ is a rigid wall and the fluid is at rest at $y = +\infty$. The linearized Navier–Stokes equations are solved, and results in the form of streamline plots are shown and discussed.

1. Introduction

An irrotational source flow with radial streamlines and a velocity diminishing with distance r from the origin like r^{-2} in three dimensions or r^{-1} in two dimensions is a solution of the equations of motion of a viscous or non-viscous fluid. If the fluid is non-viscous, this solution is also valid when the source is situated on a rigid plane wall across which no fluid passes, but along which fluid flows. Hence we can use such source flows to construct models for flows of inviscid fluid through small holes in a wall (see e.g. Tuck 1969).

On the other hand, if the fluid is viscous and cannot slip along the wall, an irrotational source flow cannot be the correct solution when the source is situated at a hole in the wall. It is the purpose of the present paper to present a solution for an *unsteady* two-dimensional flow caused by the presence of a line source of oscillating strength at the origin $x = y = 0$, the wall occupying the remainder of the plane $y = 0$, as sketched in figure 1. The unsteady motions treated are supposed to be small in amplitude, so that we can linearize the Navier–Stokes equations by neglecting convection, but not local inertia.

This problem has been studied partly because of its possible applications to physiological problems, where the wall is that of an artery (or of the heart itself) and the source is a model of a small hole. The flow of blood through such a hole would then be, in part, oscillatory and velocities would be small. Much work has been done (initially by Womersley 1955, but see also Fry & Greenfield 1963, and references quoted therein) on blood flow using the linearized Navier–Stokes equations. The results would appear to have been quite promising in so far as they concern unidirectional flow in straight tubes, but little work has been done on flows with more realistic geometries. The present work can be viewed as an attempt to proceed towards more general blood flow patterns.

However, no such applications are given in the present paper, which concerns itself solely with the analytical solution for the stream function, and the numerical computation of the streamline patterns. The stream function is obtained in the

form of a definite integral which is evaluated by numerical quadrature. Streamlines are traced using inverse interpolation on the stream function and are plotted at several instants of time, corresponding to decreasing strengths of the source, from fully source-like through to fully sink-like.

The resulting flow patterns are far from being irrotational. Indeed as the source diminishes in strength, closed circulating regions appear and subsequently migrate from near the wall to infinity. At an instant when the source is changing

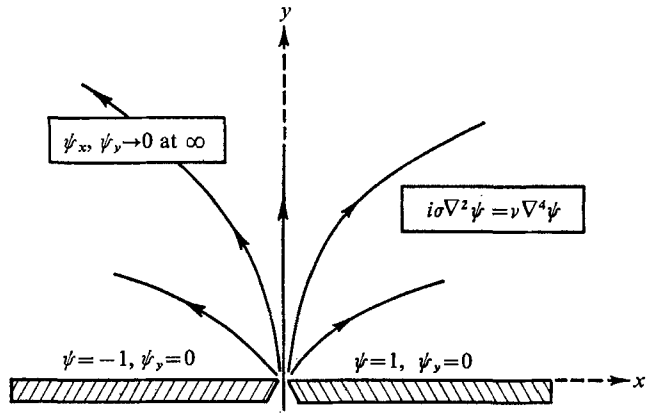

FIGURE 1

into a sink there is of course no flux from the origin at all, and the flow is entirely circulatory. Then, as the sink establishes itself, the region of closed streamlines moves outward along the symmetry plane $x = 0$ and finally disappears when the flow has become fully sink-like.

2. Formulation of the problem

We assume that the flow is two-dimensional and the fluid incompressible. Hence there exists a stream function $\psi'(x, y, t)$ such that the velocity components are

$$u = \psi'_y, \quad v = -\psi'_x. \tag{2.1}$$

The vorticity has only a z component, namely

$$\omega' = -\nabla^2\psi', \tag{2.2}$$

which satisfies the vorticity form of the Navier–Stokes equation, i.e.

$$\omega'_t + u\omega'_x + v\omega'_y = \nu\nabla^2\omega'. \tag{2.3}$$

Assuming that the amplitude of the oscillatory motion is small, we neglect the second-order convection terms on the left of (2.3), leaving the linearized equation

$$\omega'_t = \nu\nabla^2\omega', \tag{2.4}$$

or, in terms of the stream function,

$$\frac{\partial}{\partial t}\nabla^2\psi' = \nu\nabla^4\psi'. \tag{2.5}$$

The extent of validity of this approximation may be tested by an elaborate order of magnitude analysis (see e.g. Wang 1966); however, it is clear that as the amplitude of velocity fluctuations tends to zero this approximation will get better and better (but not necessarily uniformly in space).

Since (2.5) and the boundary conditions (to follow) are linear, we can obtain the solution with an arbitrary time dependence from that for sinusoidal time dependence. Thus we set

$$\psi'(x, y, t) = \mathscr{R}\psi(x, y)\, e^{i\sigma t}, \tag{2.6}$$

where $\psi(x, y)$ is a complex-valued function satisfying

$$\nabla^4\psi = \alpha^2\nabla^2\psi, \tag{2.7}$$

where $\alpha^2 = i\sigma/\nu$. Similarly, the vorticity is (2.8)

$$\omega'(x, y, t) = \mathscr{R}\omega(x, y)\, e^{i\sigma t}, \tag{2.9}$$

where
$$\nabla^2\omega = \alpha^2\omega \tag{2.10}$$

and
$$\omega = -\nabla^2\psi. \tag{2.11}$$

The boundary conditions on the velocities,

$$u, v \to 0 \quad \text{as} \quad y \to +\infty \tag{2.12}$$

and
$$u, v = 0 \quad \text{on} \quad y = 0_+ \quad (x \neq 0), \tag{2.13}$$

can be written in terms of $\psi(x, y)$ as

$$\psi_x, \psi_y \to 0 \quad \text{as} \quad y \to +\infty \tag{2.14}$$

and, on $y = 0_+$, $x \neq 0$,
$$\psi_x = 0, \tag{2.15}$$

and
$$\psi_y = 0. \tag{2.16}$$

Integrating the boundary condition (2.15), we have $\psi =$ constant on $y = 0_+$, $x > 0$, with a similar condition (but a different constant) on $y = 0_+$, $x < 0$. In fact the difference between the constant values of ψ on $x > 0$ and $x < 0$ is just the magnitude of the oscillatory flux generated by the source at $x = 0$. Again, since the problem is linear, we can without loss of generality choose these constants at will, and henceforth use

$$\psi = \pm 1 \quad \text{on} \quad y = 0_+ \quad (x \gtrless 0) \tag{2.17}$$

in place of (2.15).

We can now if we wish confine attention to the first quadrant by invoking symmetry of the flow with respect to the plane $x = 0$, and setting

$$\psi = \nabla^2\psi = 0 \quad \text{on} \quad x = 0_+ \quad (y > 0). \tag{2.18}$$

If (2.18) is used, we need only part of (2.17), namely

$$\psi = 1 \quad \text{on} \quad y = 0_+ \quad (x > 0).$$

Thus, in summary, the problem is to find ψ satisfying (2.7) in $x > 0$, $y > 0$, subject to the boundary conditions (2.14), (2.16), (2.18) and (2.19). This problem is illustrated diagrammatically in figure 1.

3. Solution for the stream function

The boundary-value problem formulated in § 2 may be solved by standard methods, such as Fourier-sine transformation with respect to x. The resulting expression for the stream function is

$$\psi = -\frac{2}{\pi\alpha^2}\int_0^\infty (\lambda+\beta)\,[\lambda\, e^{-\beta y} - \beta\, e^{-\lambda y}]\sin\lambda x\,\frac{d\lambda}{\lambda}, \tag{3.1}$$

where

$$\beta^2 = \alpha^2 + \lambda^2, \quad \mathscr{R}\beta > 0. \tag{3.2}$$

To verify that this is indeed the correct solution, we first calculate the vorticity

$$\omega = \frac{2}{\pi}\int_0^\infty (\lambda+\beta)\, e^{-\beta y}\sin\lambda x\, d\lambda \tag{3.3}$$

using (2.11), and observe that this expression satisfies (2.10) if β is given by (3.2). Hence ψ as given by (3.1) must satisfy the field equation (2.7). The boundary conditions (2.14), (2.16) and (2.18) are seen to be satisfied by inspection, while in order to test the final boundary condition (2.19) we evaluate

$$\begin{aligned}\psi(x, 0_+) &= \frac{2}{\pi\alpha^2}\int_0^\infty \frac{(\lambda+\beta)(\lambda-\beta)}{\lambda}\sin\lambda x\, d\lambda \\ &= \frac{2}{\pi}\int_0^\infty \frac{\sin\lambda x}{\lambda}\, d\lambda \\ &= 1,\end{aligned}$$

as required.

Two other forms for ψ are of interest. If we define polar co-ordinates (r, θ) by

$$x = r\cos\theta,$$

$$y = r\sin\theta,$$

then we can manipulate the formula (3.1) into the form

$$\psi = 1 - \frac{2}{\pi}\theta - \frac{2}{\pi\alpha^2}\int_0^\infty (\lambda+\beta)\,(e^{-\beta y} - e^{-\lambda y})\sin\lambda x\, d\lambda, \tag{3.4}$$

and, further, to

$$\psi = 1 - \frac{2}{\pi}\theta + \frac{2}{\pi\alpha^2}\frac{\sin 2\theta}{r^2} + \frac{2}{\pi\alpha^2}\int_0^\infty \beta\, e^{-\lambda y}\sin\lambda x\, d\lambda - \frac{\omega}{\alpha^2}, \tag{3.5}$$

where ω is the vorticity, given by (3.3).

Equation (3.4) shows ψ to be the sum of an irrotational expression $1-(2/\pi)\theta$ which satisfies the boundary conditions (2.14), (2.17), but not the no-slip condition (2.16) and is exactly the stream function for a source in an inviscid fluid, plus a rotational term which vanishes on $y = 0$. In (3.5) we have separated off some additional irrotational terms, leaving the contribution $-\omega/\alpha^2$ as the only rotational part. In fact, the harmonic function conjugate to $\psi + \omega/\alpha^2$ can be identified with the fluid pressure amplitude.

Further manipulation of the integrals in the expressions for ψ and ω is possible, and these integrals can be written, at least in part, in terms of certain Bessel and

Struve functions of complex argument. However, such manipulation serves little purpose, since values for ψ are obtained easily enough by direct numerical evaluation of the integrals. Results of such calculations are shown in the form of streamline plots in figures 2–7; discussion of these figures is postponed till § 7, after we have investigated the asymptotic properties of the flow both far from and near to the source.

4. Far-field behaviour of the flow

At a great distance from the wall $y = 0$, we should expect the flow to differ little from that for a source in an inviscid fluid. The analysis required to prove this is not difficult. Large y in the integrals corresponds broadly to small λ, and we can obtain a valid asymptotic expansion by expanding everything but the exponentials for small λ. Thus, in the expression (3.3) for the vorticity, we have

$$\begin{aligned}\omega &= \frac{2}{\pi}\int_0^\infty (\lambda + (\lambda^2+\alpha^2)^{\frac{1}{2}})\, e^{-(\lambda^2+\alpha^2)^{\frac{1}{2}}y} \sin\lambda x\, d\lambda \\ &\to \frac{2}{\pi}\int_0^\infty \{\lambda+\alpha+(\lambda^2/2\alpha)+\ldots\}\exp\{-(\alpha+(\lambda^2/2\alpha)+\ldots)\,y\}\,(\lambda x - \tfrac{1}{6}\lambda^3 x^3+\ldots)\,d\lambda \\ &= \frac{2}{\pi}\alpha^2\frac{x}{y}e^{-\alpha y}\{1+O(1/y)\}. \end{aligned} \tag{4.1}$$

Although this expression is not uniformly valid if x is also large, it remains true that for *all* x, $\omega \to 0$ *exponentially* as $y \to \infty$.

Similarly, the integral occurring in the expression (3.5) for ψ is

$$\begin{aligned}\int_0^\infty (\lambda^2+\alpha^2)^{\frac{1}{2}} e^{-\lambda y}\sin\lambda x\, d\lambda &\to \alpha\int_0^\infty e^{-\lambda y}\sin\lambda x\, d\lambda + \frac{1}{2\alpha}\int_0^\infty \lambda^2 e^{-\lambda y}\sin\lambda x\, d\lambda + \ldots \\ &= \frac{\alpha x}{x^2+y^2} + \frac{1}{2\alpha}\frac{\partial^2}{\partial y^2}\left(\frac{x}{x^2+y^2}\right)+\ldots \\ &= \frac{\alpha\cos\theta}{r} - \frac{1}{\alpha}\frac{\cos 3\theta}{r^3} + O(r^{-5}). \end{aligned} \tag{4.2}$$

This expression is uniformly valid with respect to x. Hence the asymptotic expansion of the stream function for large y is

$$\begin{aligned}\psi \to \left[1-\frac{2}{\pi}\theta\right] + \left[\frac{2}{\pi\alpha}\frac{\cos\theta}{r}\right] + \left[\frac{2}{\pi\alpha^2}\frac{\sin 2\theta}{r^2}\right] - \left[\frac{2}{\pi\alpha^3}\frac{\cos 3\theta}{r^3}\right] + O(r^{-4}) \\ + \text{exponentially small terms from } \omega. \end{aligned} \tag{4.3}$$

The leading term is of course the harmonic source stream function, while the second term can be interpreted as a dipole, the third a quadrupole, etc.

In fact we can further interpret the dipole contribution as a change of origin. Before doing this, it is best to revert to the real-valued quantity ψ' by (2.6). Thus

$$\psi'(x,y,t) = \cos\sigma t\,\mathscr{R}\psi(x,y) - \sin\sigma t\,\mathscr{I}\psi(x,y) \tag{4.4}$$

$$\begin{aligned}&\to \cos\sigma t\left[1-\frac{2}{\pi}\theta+\frac{2}{\pi}\left(\frac{\nu}{2\sigma}\right)^{\frac{1}{2}}\frac{\cos\theta}{r}+O(r^{-3})\right] \\ &\quad + \sin\sigma t\left[\frac{2}{\pi}\left(\frac{\nu}{2\sigma}\right)^{\frac{1}{2}}\frac{\cos\theta}{r}+\frac{2\nu}{\pi\sigma}\frac{\sin 2\theta}{r^2}+O(r^{-3})\right]. \end{aligned} \tag{4.5}$$

At 0° phase, i.e. $\sigma t = 0, 2\pi, \ldots$, the first square bracket in (4.5) dominates, and we can write

$$\psi'(x,y,0) = 1 - \frac{2}{\pi}\theta + \frac{2}{\pi}\left(\frac{\nu}{2\sigma}\right)^{\frac{1}{2}}\frac{\cos\theta}{r} + O(r^{-3})$$

$$= 1 - \frac{2}{\pi}\arctan\left(\frac{y-(\nu/2\sigma)^{\frac{1}{2}}}{x}\right) + O(r^{-3}), \tag{4.6}$$

i.e. the appearance of the flow at infinity is that of a source at $(0, (\nu/2\sigma)^{\frac{1}{2}})$. The streamlines will therefore ultimately be radial lines emanating from this point. For instance, the streamlines shown in figure 2 have precisely this character, and the computed angles agree well with that predicted by (4.6).

Similarly at 90° phase, i.e. $\sigma t = \frac{1}{2}\pi, \frac{5}{2}\pi$, etc., the dipole term will dominate, giving

$$\psi'\left(x, y, \frac{\pi}{2\sigma}\right) = \frac{2}{\pi}\left(\frac{\nu}{2\sigma}\right)^{\frac{1}{2}}\frac{\cos\theta}{r} + \frac{2\nu}{\pi\sigma}\frac{\sin 2\theta}{r^2} + O(r^{-3}). \tag{4.7}$$

Again, the $O(r^{-2})$ term can be interpreted as a change of origin, this time to $(0, (2\nu/\sigma)^{\frac{1}{2}})$, and the streamline pattern approximates to circles through this point tangent to the plane $x = 0$. The computed streamlines shown in figure 5 confirm this asymptotic analysis. At phases other than multiples of 90°, some streamlines will be ultimately radial, while others will be dipole-like near infinity.

5. Near-field behaviour of the flow

The detailed asymptotic analysis of the integrals when $r = (x^2+y^2)^{\frac{1}{2}}$ is small is quite difficult. One can obtain the first few terms by expanding for *large* λ while keeping $\lambda x, \lambda y$ bounded. Thus, from (3.4) we have

$$\psi = 1 - \frac{2}{\pi}\theta - \frac{2}{\pi\alpha^2}\int_0^\infty \left(\lambda + \lambda + \frac{\alpha^2}{2\lambda} + \ldots\right)(e^{-\lambda y}\exp\{-(\alpha^2 y/2\lambda)\}e^{-} \ldots - e^{-\lambda y})\sin\lambda x\, d\lambda$$

$$= 1 - \frac{2}{\pi}\theta + \frac{2y}{\pi}\int_0^\infty \left[1 - \frac{\alpha^2 y}{4\lambda} + \ldots\right] e^{-\lambda y}\sin\lambda x\, d\lambda$$

$$= 1 - \frac{2}{\pi}\theta + \frac{2y}{\pi}\frac{x}{x^2+y^2} - \frac{2y}{\pi}\cdot\frac{\alpha^2 y}{4}(\tfrac{1}{2}\pi - \theta) + \ldots$$

$$= \left[1 - \frac{2}{\pi}\theta + \frac{\sin 2\theta}{\pi}\right] - \tfrac{1}{4}\alpha^2 r^2 \sin^2\theta\left(1 - \frac{2}{\pi}\theta\right) + O(r^4). \tag{5.1}$$

The above analysis is somewhat less than rigorous, but a more refined asymptotic expansion leads to the same result and to the error term $O(r^4)$ shown.

The correctness of the expansion (5.1) may, however, be independently verified by reference to the original boundary-value problem. If we look at the near-field approximation of the field equation (2.7) (e.g. by stretching coordinates with respect to some artificial small parameter) it is clear that the limiting form of (2.7) is the biharmonic equation. That is, if for small r

$$\psi(x,y) \to \psi_0(x,y) + \psi_1(x,y) + \ldots, \tag{5.2}$$

where terms are of decreasing order of magnitude with respect to r, then the leading term ψ_0 must satisfy

$$\nabla^4\psi_0 = 0, \tag{5.3}$$

and the second term ψ_1 satisfies

$$\nabla^4\psi_1 = \alpha^2\nabla^2\psi_0. \tag{5.4}$$

It is readily verifiable that the function

$$\psi_0 = 1-\frac{2}{\pi}\theta+\frac{\sin 2\theta}{\pi} = \psi_0(\theta) \tag{5.5}$$

is indeed a solution of the biharmonic equation (5.3) and satisfies the boundary conditions (2.15)–(2.18), while

$$\psi_1 = -\tfrac{1}{4}\alpha^2 r^2\sin^2\theta\left(1-\frac{2}{\pi}\theta\right) \tag{5.6}$$

satisfies (5.4) and vanishes with its normal derivative on $y = 0$. The solution (5.5) was obtained by Rayleigh (1893) in solving a Stokes-flow problem.

One is more used to this Stokes-type approximation in the case of creeping flows, and it is perhaps surprising to find that in the present flow the Stokes approximation is valid in the region of *greatest* velocities, near the origin. However, it should be observed that the flow represented by $\psi_0(\theta)$, although radial, is very different from that of a harmonic source. The streamlines associated with ψ_0 are crowded near to $\theta = \frac{1}{2}\pi$ (see e.g. figure 2), and no flow at all takes place along the wall $\theta = 0$. Hence not only are the velocities large, but the shear is also very large, so large as to cause the viscous terms in the equation of motion to dominate the local inertia terms.

Expressing the result (5.1) in terms of the real stream function $\psi'(x, y, t)$, we have

$$\psi'(x,y,t) = \cos\sigma t\left[1-\frac{2}{\pi}\theta+\frac{\sin 2\theta}{\pi}\right]+\sin\sigma t\left[\frac{\sigma}{4\nu}r^2\sin^2\theta\left(1-\frac{2}{\pi}\theta\right)\right]+O(r^4).$$

Thus at zero phase, streamlines near the origin are radial (but crowded near $\theta = \frac{1}{2}\pi$, as mentioned above) whereas at 90° phase the streamlines are solutions of $r^2\sin^2\theta\{1-(2/\pi)\theta\}$ = constant. These curves are concave upwards, looking much like hyperbolae. In combination with the concave-downward dipole-like far-field behaviour of these streamlines, this suggests closed streamlines. The necessity for closed streamlines at 90° phase is further indicated by the fact that $\psi'(x, y, \pi/2\sigma)$ tends to zero *both* as $r \to 0$ and $r \to \infty$, so that no streamline can end at the origin or at infinity. In fact all streamlines at 90° phase are closed (figure 5); for phases other than multiples of 90° some streamlines must be closed, while others go from $r = 0$ to $r = \infty$.

6. Numerical analysis

Before evaluating the stream function numerically, it is convenient to non-dimensionalize by writing in (3.1) and elsewhere,

$$\left.\begin{aligned} x' &= x(\sigma/\nu)^{\frac{1}{2}},\\ y' &= y(\sigma/\nu)^{\frac{1}{2}},\\ \lambda' &= \lambda(\nu/\sigma)^{\frac{1}{2}},\end{aligned}\right\} \tag{6.1}$$

etc., and immediately dropping the dashes. The net effect of these transformations is simply to replace α^2 by i wherever it occurs; i.e. the frequency σ and viscosity ν appear only in the form of a length scale $(\nu/\sigma)^{\frac{1}{2}}$ which is absorbed into the co-ordinates.

In particular, (3.1) becomes

$$\psi(x,y) = -\frac{2}{\pi i}\int_0^\infty (\lambda+(\lambda^2+i)^{\frac{1}{2}})\left[e^{-y(\lambda^2+i)^{\frac{1}{2}}} - \frac{(\lambda^2+i)^{\frac{1}{2}}}{\lambda}e^{-\lambda y}\right]\sin\lambda x\, d\lambda. \quad (6.2)$$

Numerical values of the stream function were obtained by direct trapezoidal approximation of (6.2), giving

$$\psi(x,y) \simeq -\frac{2}{\pi i}\Delta\lambda \sum_{j=1}^{N} (\lambda_j+\beta_j)\left(e^{-\beta_j y} - \frac{\beta_j}{\lambda_j}e^{-\lambda_j y}\right)\sin\lambda_j x, \quad (6.3)$$

where
$$\lambda_j = j\Delta\lambda \quad (6.4)$$

and
$$\beta_j = (\lambda_j^2+i)^{\frac{1}{2}}. \quad (6.5)$$

The calculations were performed on a CDC 6400 computer, using the complex arithmetic facility of FORTRAN IV.

The accuracy of the approximation (6.3) depends on the two parameters $\Delta\lambda$, the fineness of subdivision, and N, the number of terms summed. Both of these parameters were chosen automatically in order to achieve 4 significant figure accuracy no matter what the value of x or y. For instance, when y is small, N is taken at least large enough for the exponentials to be less than 0·00005, i.e.

$$N > \frac{10}{\Delta\lambda.y}. \quad (6.6)$$

On the other hand, when x is large, $\Delta\lambda$ must be small enough for $\sin\lambda x$ not to vary too rapidly over one interval $\Delta\lambda$. Thus, for $x > 1$,

$$\Delta\lambda < \epsilon/x, \quad (6.7)$$

where ϵ is an interval small enough to achieve 4-figure accuracy at $x = 1$ (found by trial and error). Other criteria were built into the production program, which did in fact achieve a uniform 4-figure accuracy, tested by comparison with a corresponding 6-figure program.

The streamlines shown in figures 2–7 were obtained in the simplest possible way by inverse interpolation on $\psi'(x,y,t)$. For instance, at fixed values of x and ψ' we can interpolate to find the value of y at which the streamline $\psi' =$ constant crosses the line $x =$ constant. Inverse interpolation with respect to the polar co-ordinate θ, at fixed r, was also used. The interpolation process was continued iteratively, usually taking only one or two cycles, until the value of ψ' was within 0·0005 of that demanded, or, in a case where the streamline did not cross the given line $x =$ constant, until failure to find the streamline was apparent.

The procedures described above were developed with the primary aim of minimizing expenditure of the author's time, not necessarily that of the computer, while maintaining a strict control on the accuracy of the results. Nevertheless, only about 1 h of central processor time was required in total for the production runs leading to figures 2–7, so that a search for more efficient numerical methods would have been wasteful.

7. Discussion of computed streamlines

Figures 2–7 show the development of the streamline patterns with time, starting from $\sigma t = 0$ when the maximum outflow is occurring, moving through $\sigma t = \frac{1}{4}\pi$ (45° phase, source half turned off) and $\sigma t = \frac{5}{12}\pi$ (75° phase) to $\sigma t = \frac{1}{2}\pi$ (90° phase, turned off), and then as the flow becomes inward or sink-like, through

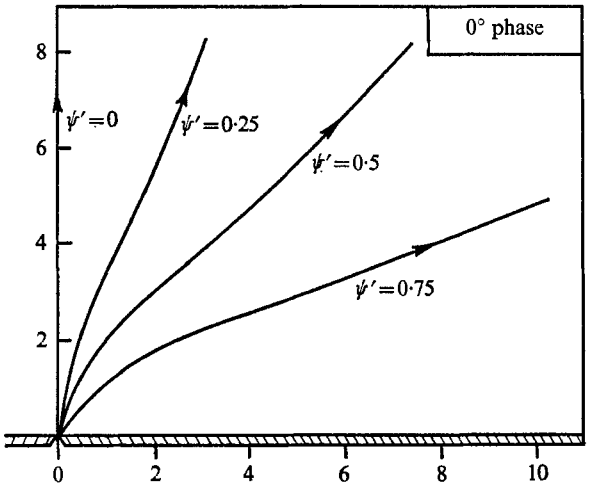

FIGURE 2

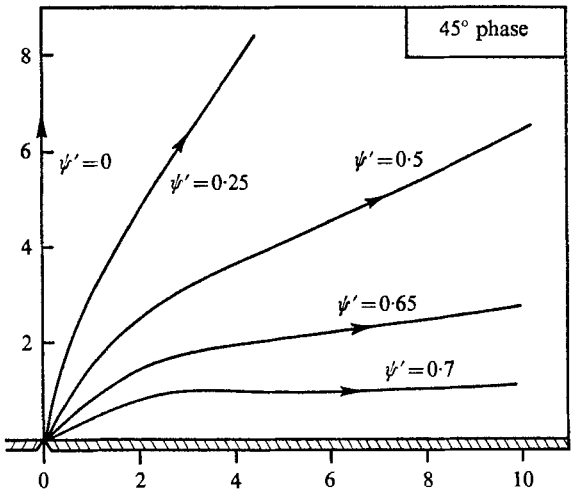

FIGURE 3

$\sigma t = \frac{7}{12}\pi$ (105° phase) to $\sigma t = \frac{3}{4}\pi$ (135° phase, sink half turned on). The streamlines at $\sigma t = \pi$ (180° phase, flow fully sink-like) are not shown, as they are identical to those of figure 2 with reversed direction.

The fully source-like streamlines of figure 2 all emanate from the origin and end at infinity. The fluid particles avoid moving near the fixed wall $y = 0$, so that as they emerge from the origin they are biased towards the vertical. The computed

nearly straight portions near the origin agree with the asymptotic analysis of § 5, as do the far-field portions with § 4. To within the order of accuracy of the figure, the near-field result seems to be valid for $r < 1$ and the far-field for $r > 4$, remembering that the co-ordinates plotted are made non-dimensional with respect to $(\nu/\sigma)^{\frac{1}{3}}$.

As soon as the strength of the source starts to diminish it would appear that closed streamlines form. A closed bubble-like region of circulating fluid appears

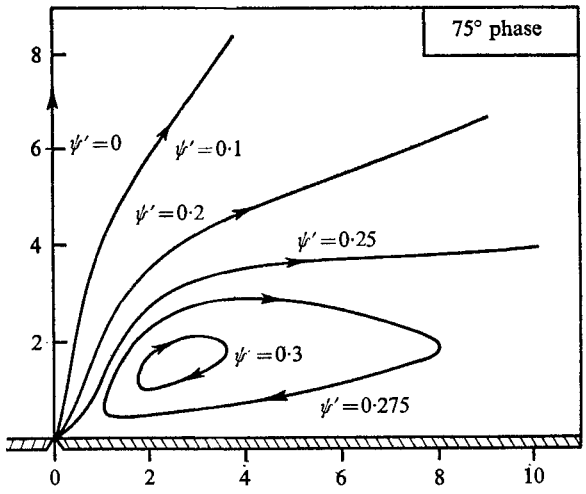

FIGURE 4

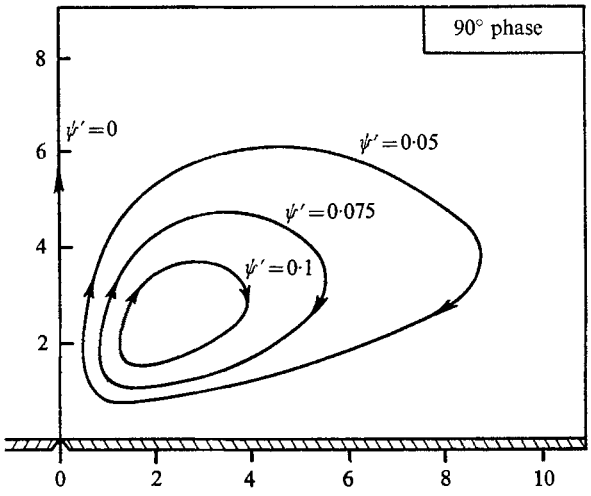

FIGURE 5

near the origin and grows in size. At 45° phase (figure 3) such a region no doubt occurs near (3·0, 0·5), although it would have been quite difficult to find and plot it using the present program. The value of ψ' on $y = 0$ is $\cos\frac{1}{4}\pi$ or 0·707, so that the streamline $\psi' = 0{\cdot}7$ shown leaves very little 'space' in flux for more streamlines, even though it has a substantial upward bump at $x = 3{\cdot}0$. On the

other hand, at 75° phase (figure 4) the region of circulating fluid has become quite apparent. Here the value of ψ' on $y = 0$ is 0·26, and any streamline with ψ' greater than this, such as $\psi' = 0{\cdot}275$ and $\psi' = 0{\cdot}3$, must be closed.

When we reach 90° phase (figure 5), the strength of the source has dropped to zero, and no fluid is actually leaving the origin at all. What remains is a mass of

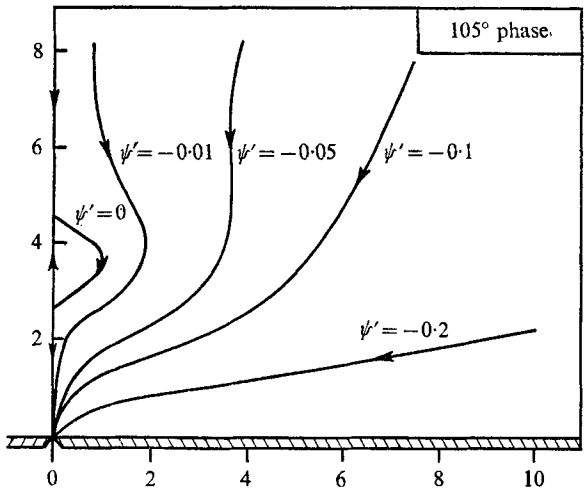

FIGURE 6

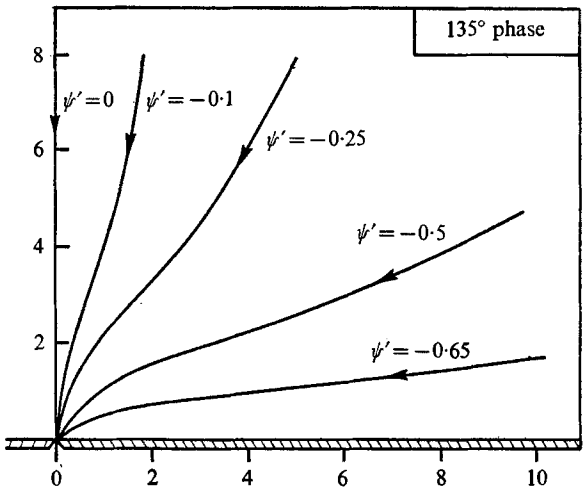

FIGURE 7

circulating fluid, the direction being clockwise and the value of the stream function small but positive. The maximum value of ψ' appears to be about 0·15, the centre of the region being at about (3·0, 3·0).

Now as time further increases the flow becomes sink-like, the lower left-hand parts of the closed streamlines of figure 5 being drawn into the origin. The remaining circulatory flow is thrown upward, creating (figure 6) a bubble-like region centred on $x = 0$. The existence of this region at 105° phase is indicated

by the fact that ψ' can be zero at points not on $x = 0$. Thus the symmetry streamline $\psi' = 0$ divides on $x = 0$.

Finally, at 135° phase (figure 7) the closed region has moved upward and is out of the graph shown (although it would in any case be too small and elongated to plot). The flow is now strongly sink-like and becomes fully sink-like at 180° phase. This picture of the flow now repeats itself, the sink turning off and a source re-establishing itself.

REFERENCES

FRY, D. L. & GREENFIELD, J. C. 1963 The mathematical approach to hemodynamics, with particular reference to Womersley's theory. *Pulsatile Blood Flow* (ed. E. O. Attinger). Ch. 4. New York: McGraw-Hill.

RAYLEIGH, LORD 1893 On the flow of viscous liquids, especially in two dimensions. *Phil. Mag.* (5), **36**, 354.

TUCK, E. O. 1969 Transmission of water waves through small apertures. (Unpublished.)

WANG, C-Y. 1966 The resistance on a circular cylinder in an oscillating stream. *Quart. Appl. Math.* **23**, 305.

WOMERSLEY, J. R. 1955 Oscillatory motion of a viscous liquid in a thin-walled elastic tube. I. The linear approximation for long waves. *Phil. Mag.* **46**, 199.